Bulletin of the Mineral Research and Exploration

http://bulletin.mta.gov.tr

Landslide susceptibility mapping using information value and frequency ratio for the Arzew sector (North-Western of Algeria)

Roukh ZINE EL ABIDINE[a*] and Nadji ABDELMANSOUR[a]

[a]*Laboratory of Geo resources, Environments and Natural Risks, Oran 2 Mohamed Benahmed University, Faculty of Earth Science and the universe, B.P1 1524 El-M'Naouar. Oran31000. Algeria.*

Research Article

Keywords:
Landslide susceptibility mapping, Frequency Ratio, Information value, Arzew, Algeria.

ABSTRACT

Geological hazards present one of the most important constraints for the development of the Arzew sector (Oran province), North Western of Algeria. Landslides are considered us one of the most common phenomena in the study area and especially in the hilly area. For minimizing and reducing the consequences of this problem, it is necessary to carry out preliminary studies on the cartography of the different zones exposed to the slope instability phenomena. The main objective of this study is to perform the landslide susceptibility mapping by statistical models and GIS techniques for the Arzew area. To achieve this goal, an analytical approach was carried out. Firstly, a landslide inventory map was prepared using previous inventory maps, satellite images, aerial photos and field surveys. Secondly seven conditioning factors such as slope degree, aspect, lithology, land use, distance to the streams, distance to the road and altitude were exploited to assess landslide susceptibility. Thirdly, the weight value for each class of the conditioning factors was determined using Frequency Ratio (FR) and Information Value (IV) models based in GIS functionalities. Consequently, Landslide Susceptibility Maps (LSMs) were produced by the classification process of the global Landslide Susceptibility Indexes (LSIs) into five classes. Finally, for experiment verification, the LSMs obtained with the FR and IV models were confirmed comparing LSMs with landslide inventory map using both the Receiver Operating Characteristics (ROC) and the Seed Cell Area Index (SCAI) models. The area under curve (AUC) results, demonstrate that the IV method more performance (89.03%) for LSM than FR method (85.57%). Furthermore, the validation results using SCAI also confirmed that the IV model was more accurate than FR model. The models employed in this study are capable to resolve the issue of the landslide susceptibility of the study area. The produced susceptibility maps can be used for future land use planning and can be considered as a powerful tool to resolve the spatial distribution of the risk associated to landslides.

Received Date: 02.05.2018
Accepted Date: 22.10.2018

1. Introduction

Landslides was considered one of the most frequent and damaging natural hazards threatening the human lives, economic, big projects and properties in northern part of Algeria (Benaissa et al., 1989; Guemache et al., 2011; Hadji et al., 2017; Djerbal et al., 2017). Oran region, located in north western of Algeria, known for its complex geology (recent tectonic and seismic activity), is particularly exposed to the landslide hazard. To minimize landslides consequences, it requires a rational land use in the spatial planning. As a solution, landslide susceptibility maps were considered the principal tool for predicting risk.

The susceptibility to landslides is the probability of spatial occurrence of the landslide for several factors

Citation info: Zine El Abidine, R., Abdelmansour, N. 2019. Landslide susceptibility mapping using information value and frequency ratio for the Arzew sector (North-Western of Algeria). Bulletin of the Mineral Reserach and Exploration, 160, 197-211. *https://doi.org/10.19111/bulletinofmre.502343*

* *Corresponding author: Roukh ZINE EL ABIDINE, zinougeorisque@gmail.com*

of environmental predisposition (slope, aspect, land use, lithology, etc) for a given area (Thiery, 2007; Guzzetti et al., 2005). The GIS techniques are the most important tools enable quickly generate this type of thematic maps.

The landslide susceptibility mapping can be estimated by the use of several methods based on GIS techniques. Many studies have used frequency ratio for assessing landslide susceptibility such as (Akgün et al., 2008; Yalçın et al., 2011; Youssef et al., 2015). Other studies have used Logistic regression model to evaluate landslide susceptibility (Gorsevski et al., 2006*b*; Yılmaz, 2010; Bai et al., 2011; Pourghasemi et al., 2013; Raja et al., 2017). The statistical index model (information value) is also used to resolve the thematic of landslide susceptibility (Bui et al., 2011; Cui et al., 2016; Aghdam et al., 2016). The weight of evidence model has also used by many researches (Regmi et al., 2010; Özdemir and Altural, 2013). The analytical hierarchy process (AHP) (Gorsevski et al., 2006*c*; Ercanoglu et al., 2008; Intarawichian and Dasananda, 2010; Chen et al., 2016; Ghosh et al., 2017), fuzzy set (Pradhan, 2011; Sezer et al., 2011), the Support Vector Machine (SVM) method (Ballabio and Sterlacchini, 2012; Peng et al., 2014; Pradhan et al., 2017) and artificial neural network (Yılmaz, 2009; Conforti et al., 2014; Chen et al., 2017) were applied to the landslide hazard zoning.

In Algeria, landslide susceptibility mapping presents a novel approach for prevention of the risks linked to the landslides. So far, few attempt at landslide susceptibility were applied in Algeria (Hadji et al., 2013; Djerbal and Melbouci, 2013; Hadji et al., 2014; Bourenane et al., 2015; Achour et al., 2017; Hadji et al., 2017; Dahoua et al., 2017; Mahdadi et al., 2018).

Landslide susceptibility zonation is indispensable for land-use management and should become an official document for various future projects (Gorsevski et al., 2006a; Corominas et al., 2014). The geographical position of the study area has the particularity of being an economic and tourism ultimate center, requires preliminary studies in the planning and risks management. To define landslide prone area, the present research destined to mapping landslide susceptibility for the Arzew sector (Northwestern of Algeria).

In this study, simple method was used to landslide susceptibility mapping, by following three essential steps: The first one consist to collect the data input, the second one, calculated the landslide susceptibility index using two models based on GIS. Step three, establishment and validation of the output data.

2. General Characteristics of the Study Area

The study area is part of the Oran coastal, northwest of Algeria, located between the UTM coordinates WGS84 zone 30 (3976894.08 m, 3954859.17 m) latitude and (715833.47 m, 747107.72 m) longitude (Figure 1), were the area of this region is 308.06 km².

The geomorphological unities of the study area is characterized by the presence of plains, mountains and plateaus, the altitude range between (0 and 625) meters on the reliefs (Figure 1). Arzew climate is part of the semi-arid Mediterranean bioclimatic stage, of which highly developed hydrographic network which has a flow conforming to the topography of the region. Towards the north, the hydrography has a flow directed towards the sea, while towards the south the superficial flow feeds several endoergic structures, represented by several lakes and sebkha (Figure 2).

The study area is part of the alpine belt, containing Paleozoic, Mesozoic, highly tectonized, largely metamorphosed units (Ciszak, 1993). According to the geological maps (Gourinard, 1952*a*,*b*) four units in the study area are made up of three apparent and distinct geological entities (Figure 3). They are distributed from east to west respectively; Kristel Mountain, Borosse and Orousse Mountains, the fourth entity presented by Djebel Essebouaa. Djebel Borosse and more complex than Djebel Orousse, both are constituted by relatively thick carbonate and calcaro-schistose formations. Milled limestones truncated by dominant erosion surfaces. Their impressive abrupt cliffs are formed by schist characterized by a overlapping structure of Neogene to Plio-Quaternary age (Perrodon, 1957; Fenet, 1975; Thomas, 1985). The Miocene subdivided into two sedimentary cycles. The first post-nappe cycle presented by green marls located between the southern flank of Djebel Essebouaa and the plateau of Boufatis for the second cycle is preceded by an active erosion phase accompanied by an accumulation of continental series to the East of Oran. Marlins and cineretic formations rely on deposits of Canastel's first post-nappe cycle (Oran cliffs - Canastel).

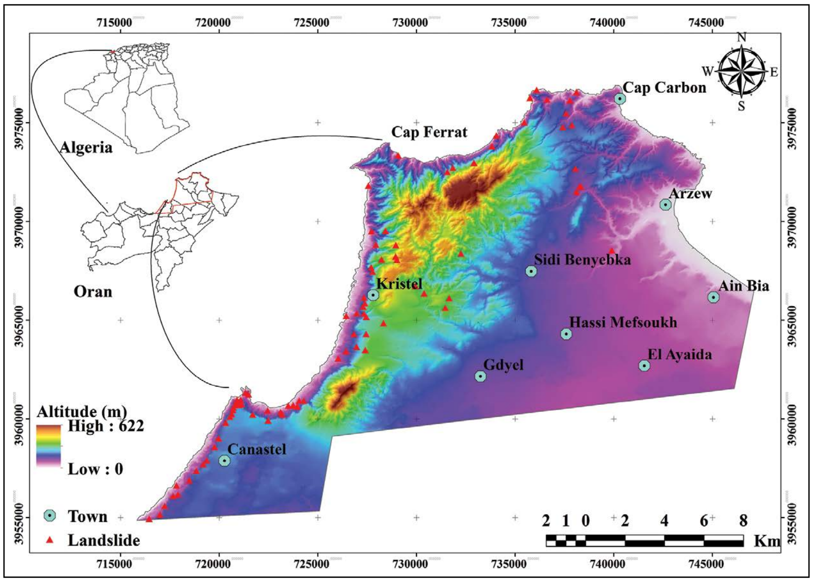

Figure 1- Location of study area.

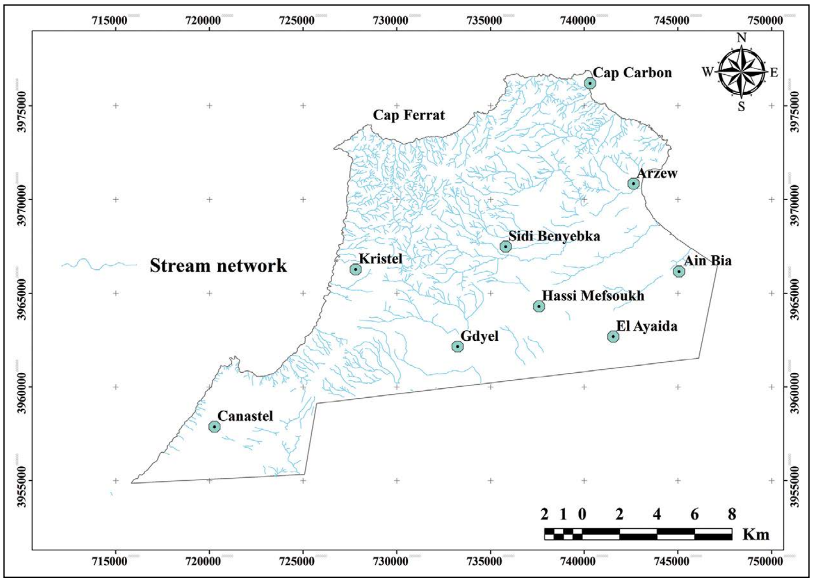

Figure 2- Streams network map of the study area.

The South and East of the Arzew massif, marked by marly outcrops and gypsum, the upper Miocene is covered by the Pliocene. The latter is often confused with the quaternary lands. The term Plio-Quaternary, which is vague and imprecise, gives rise to various confusions. In this context, we agree with Thomas 1985 nomenclature for Pliocene and Quaternary terrains: PI: represented by sandy conglomerates, marls and marine sands laterally at the foot of the schistose massifs, to continental conglomeratic deposits. These deposits are of Tabianian age. The PII cycle: it is represented by the formation of the Golf of Arzew. These lumacheles pass laterally (in some places) to sandy dunes, or marls and sands in the center of the basin (Telamine lake and Arzew salt). The Pleistocene is often formed by rube silt and gray silt with Lateral equivalents represented either by shell sands, dunes or even fluvio-lacustrine clays. A calcareous crust (pink to reddish-brown slab) develops on various facies in relation to the shaping of the ablation surfaces correlative to the deposits of type playa.

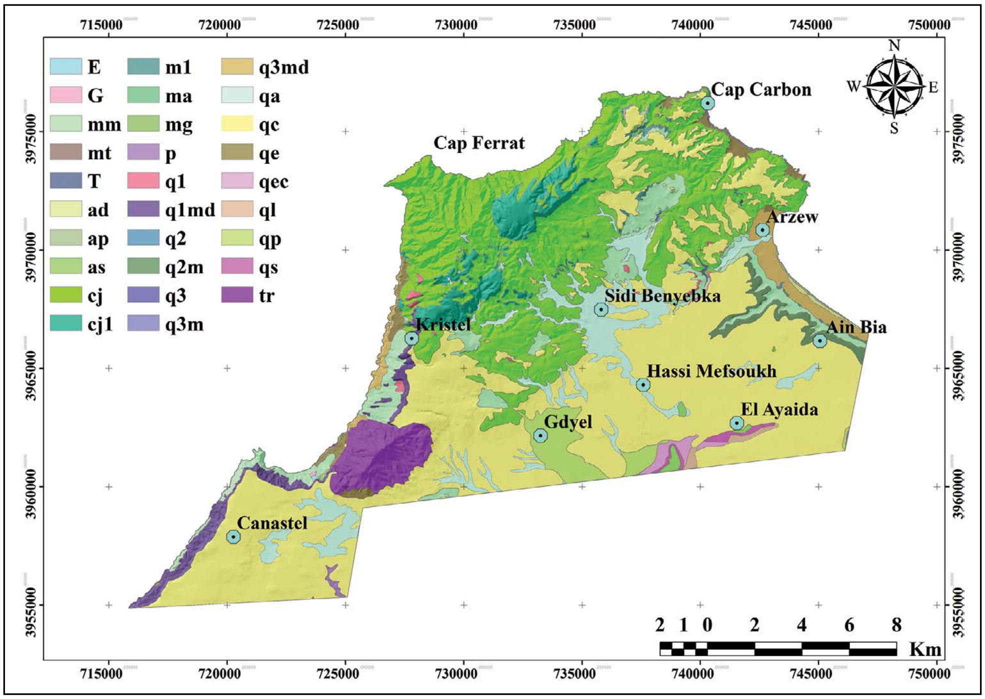

Figure 3- Lithological map of the study area, ad: dune vives, as: low salted bottoms vegetation; Ap: beach, p: marly more or less sandy; Q1: marine Pleistocene (Calabrian); Q1m: lumachelle; Q1md: dune marine; Q2: intermediate marine Pleistocene; Q2m: marine lumachelle, Q3: recent marine Pleistocene; Q3m: scallop lumachelle; Q3md: marine dune; Qa: continental quaternary associated with alluvium; Qc: carapace and topsoil more or less encrusted; Qe: eboule; Qec: carapace and topsoil more or less encrusted and collapsed; Ql: Pleistocene marine ancient level; Qp: continental quaternary (clay lake); Qs base salted bottom with vegetation; M1: algae limestone; Mm: gray marl; Mg: fine sand with yellow marl; Mt: white marl-limestone; Cj1: limestone marmorised sometimes dolomitized; Cj: schist; Tr: permo-triace (purplish schist); E: eruptive (green rocks); G: diapirism (gypsum); T source deposit (Gourinard 1952 *a*,*b*).

3. Landslide Inventory

Landslide inventory mapping is one of the key process of landslide susceptibility modeling (Fell et al., 2008; Corominas et al., 2014) . Satellites images, aerial photos, GPS, reviews, articles, internal reports and fields' survey provide important tools to establish landslide inventory map. This map contains a landslide position that arises in the past. In this study, the landslide positions were identified using existence data base, satellite images, aerial photos, Google Earth, and field surveys. Eventually, data base contains more than 80 polygons. Figure 4 illustrate the spatial distribution of landslide location in the Arzew sector, Algeria. In this study we used landslides classification developed by Cruden and Varnes 1996. Landslides are grouped into three types: rotational, translational and compound slide. Figure 5 illustrates some example of landslide affected the study area.

4. Conditioning Factors

Generally, mass movement result from the combination of triggers and aggravating factors, particularly the lithological, structural and geotechnical characteristics, slope angle, groundwater, surface water and seismic… etc. Their distribution over time is irregular and their frequency is conditioned by extreme natural events.

The conditioning-factors used in this research are slope angle, slope exposure, lithology, land use, altitude, distance to the streams and distance to the road. They are generated by different sources (Table 1). However, the topographic attributes such as slope angle, slope exposure and altitude were derived from Digital Elevation Model (DEM). The DEM was established accordingly by digitization and interpolation of the topography map curves extracted from a 1:25000 scale topographical maps

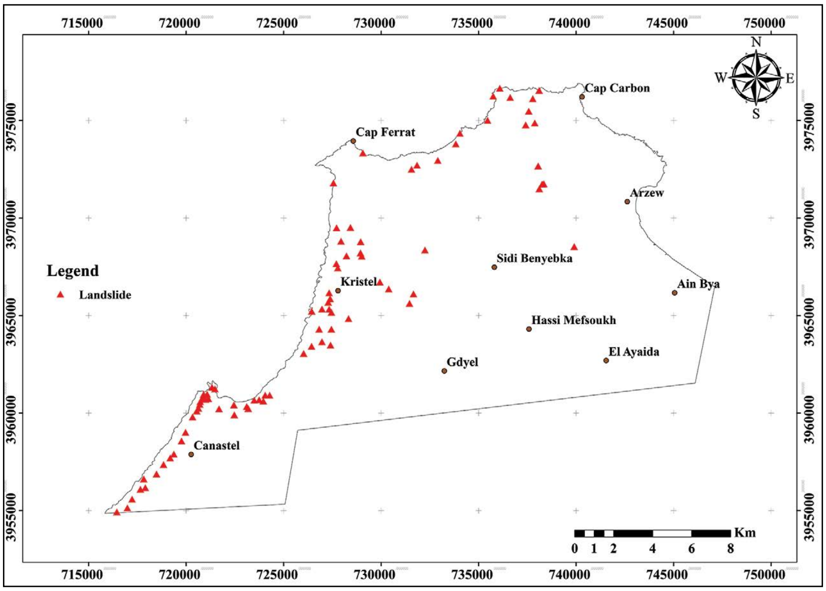

Figure 4- Landslide spatial distribution map.

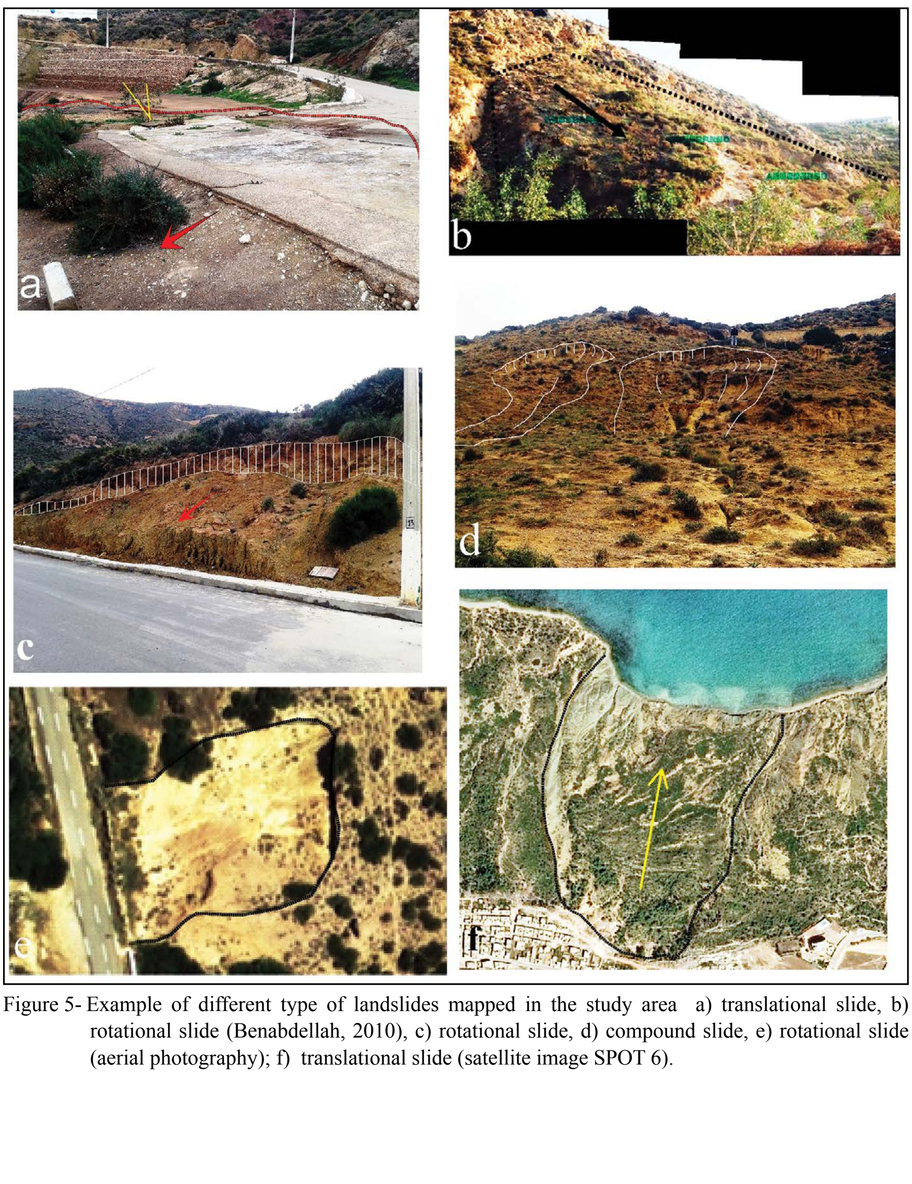

Figure 5- Example of different type of landslides mapped in the study area a) translational slide, b) rotational slide (Benabdellah, 2010), c) rotational slide, d) compound slide, e) rotational slide (aerial photography); f) translational slide (satellite image SPOT 6).

Table 1- Information source for the various parameters used in the landslides susceptibility mapping .

Setting	Maps	Sources of informations
Landslide inventory	Landslide inventory map	Satellite images (SPOT6), Google Earth, aerial photography, field surveys and bibliographic data.
Topography	DEM	Creation of DEM by digitization and interpolation the contours lines extracted from 1/25000 scale topographical maps.
Morphometric	Slope map Slope Exposure map Altitude map	Derived from DEM
Geological	Lithological map	Digitization lithological formations from 1/50000 scale geological maps
Hydrology	Distance to the streams map	Digitization the stream network from the 1/25000 scale topographic maps.
Land use	Land use map Distance to the road map	Land use map (BNEDER 2011), satellite image, field surveys.

(Figure 1), the lithology was extracted from a 1:50000 scale geological maps and furthermore the both land use map and distance to the road map are extracted from a 1:25000 scale land use map of Oran elaborated by National office of studies for rural development (Beneder, 2011), field survey and satellite images.

4.1. Slope Angle

Slope degrees allowed to increases acculturation of the slope movement, that's why this parameter presented one of the aggravating landslide factors. using DEM and GIS functions, slope degree were classified into 5 classes: 0-10°, 10-20°, 20-30°, 30-50° and >50° (Figure 6).

4.2. Slope Exposure (Aspect)

Aspect considered as the exposition of slope, it is measured clockwise in degree from 0 to 360 °, the values that are less than 1 represents flat area. Aspect also presents an essential conditioning factor in landslide susceptibility process. Figure 7 illustrates the aspect map of the Arzew sector with nine classes.

4.3. Lithology

Lithology considered the most important conditioning factor because each lithological unit has landslide susceptibility level (Yeşilnacar and Topal, 2005). In the current study, lithological map was prepared by digitization of a 1:50000 scale geological maps. Based on geotechnical and geomorphological

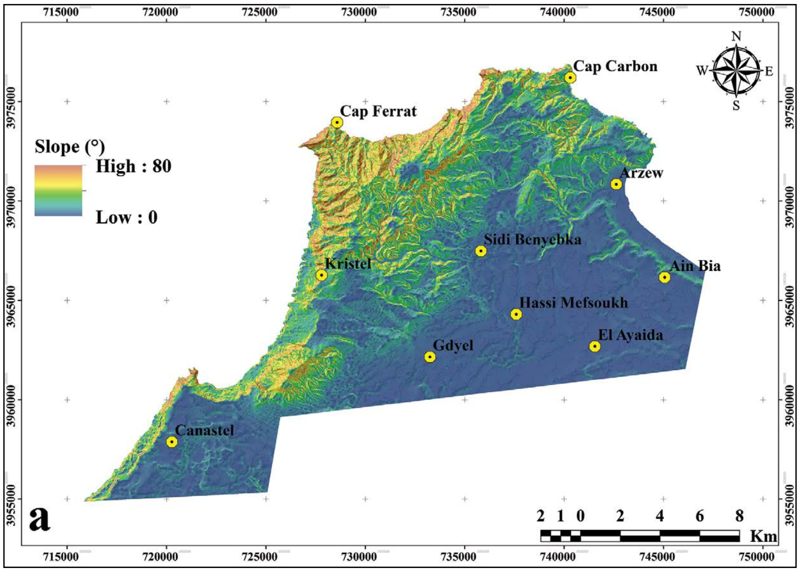

Figure 6- Slope map of the study area.

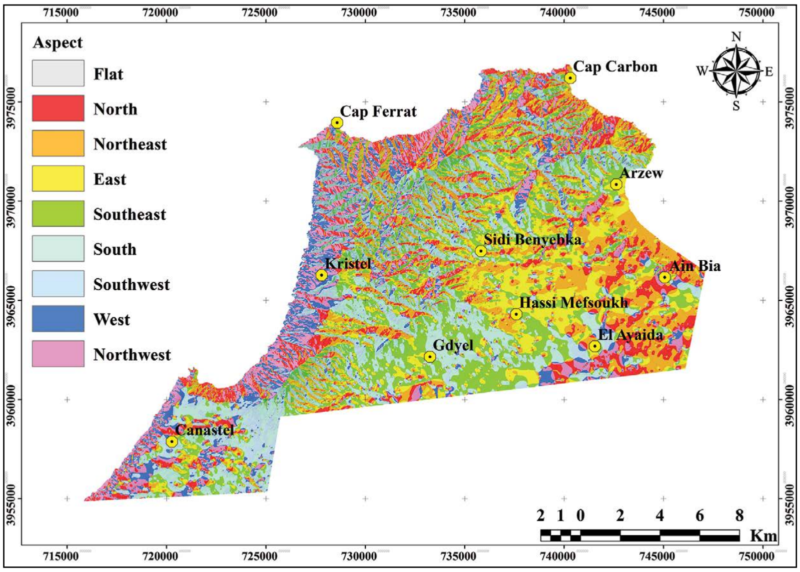

Figure 7- Aspect map of the study area.

characteristics, they were classified into four classes using ArcGIS software (Table 2).

4.4. Distance to the Streams

Generally, landslides developed near streams where flow velocity is sufficiently to erode the lower part of talus. For this distance to the streams were integrated in landslide susceptibility estimation, using Euclidean distance function in ArcGIS, streams buffer zone were established and classified in six classes (0-100, 100-200, 200-300, 300-400, 400 -500, > 500).

4.5. Land Use

Barren and little vegetative land makes talus more prone to erosion and sliding (Gomes et al. 2005), so land use considered an important parameters included in this study. Land use map of Arzew sector produced by digitization of 1/25000 scale land use map of the Oran (Figure 8), it is reclassified into four classes (Table 2).

4.6. Distance to the Road

During the road construction, the anthropogenic actions influencing landslide, and that is through by destroy vegetation, application of external loads (Bourenane et al., 2015). Accordingly, the distance to the road considered an important parameter in this study. In current study, distance to the road divided into 5 zones using an interval of 150m: (0-150, 150-300, 300-450, 450-600, >600).

4.7. Altitude

Slope movement intensity increases with altitude increasing, in this research, DEM were used to perform altitude map based on Reclassify function in Arc GIS. From 0 to 622, altitude classified into 6

Table 2- Classification of lithology and land us.

Lithology	Class1	Q3, Ad, Qs, Ql, Qa, Qc, Ap, As, P, Q2, Qec, T, Qp, Qs.
	Class2	Tr, Cj1, Cj.
	Class3	Q2m, Mg, Q3m, Q3md, Ml.
	Class4	Ma, Mt, Qe, Q1md, Mm, E, G.
Land use	Class1	Forest, Fruit crops, Olive growing, Water body.
	Class2	Maquis wooded, maquis.
	Class3	Wine-growing, Mixed cropping, Vegetable growing, big culture, urban.
	Class4	Mines, Bare soil.

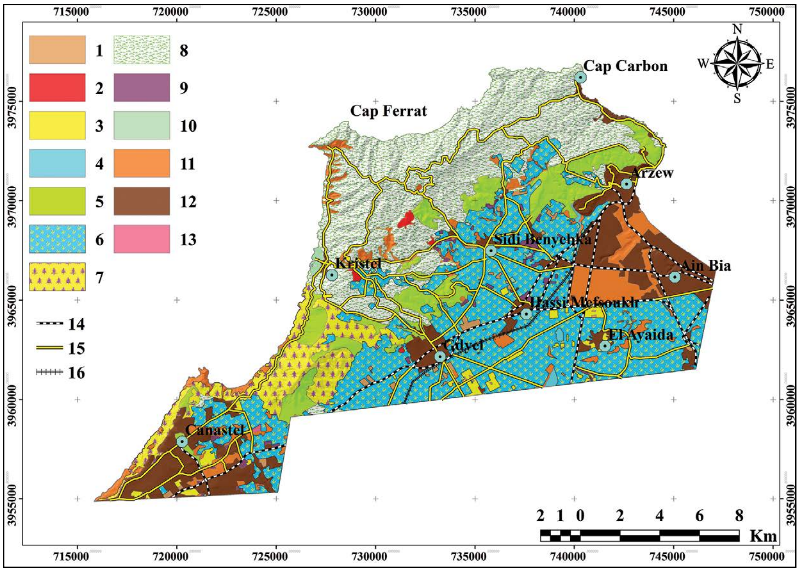

Figure 8- Land use map of study area. 1 fruit crops, 2 mines, 3 vegetable growing, 4 water body, 5 forests, 6 big culture, 7 maquis wooded, 8 maquis, 9 olive growing, 10 mixed cropping, 11 bare land, 12 urban, 13 wine-growing, 14 major road, 15 secondary road, 16 rail road.

classes: 0-100, 100-200, 200-300,300-400, 400-500 and >500 (Figure 9).

5. Landslide Susceptibility Mapping

In this paper, statistical index method and frequency ratio were applied to mapping landslide susceptibility. Weight of each causative factors class was defined by the combination of each parameter and landslide inventory map. By combination following decision rules (addition, division, multiplication …etc), weight of each conditioning factors class was defined. Finally, classification of landslide susceptibility index using natural break (jenks) and validation of landslide susceptibility maps comparing LSMs and inventory map. Figure 10 illustrates the flowchart of methodology used in this research.

5.1. Frequency Ratio Method

The fundamental concept of this method is to calculate the ratio between the density of phenomena

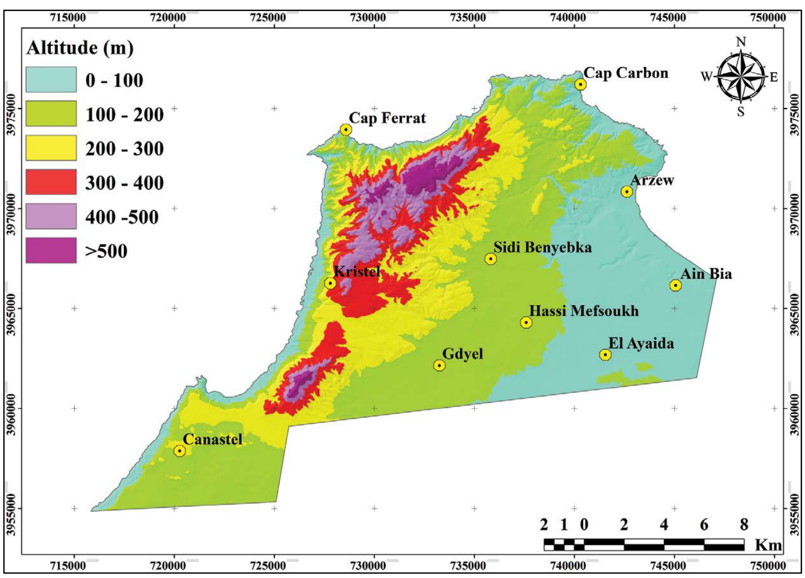

Figure 9- Altitudes map of study area.

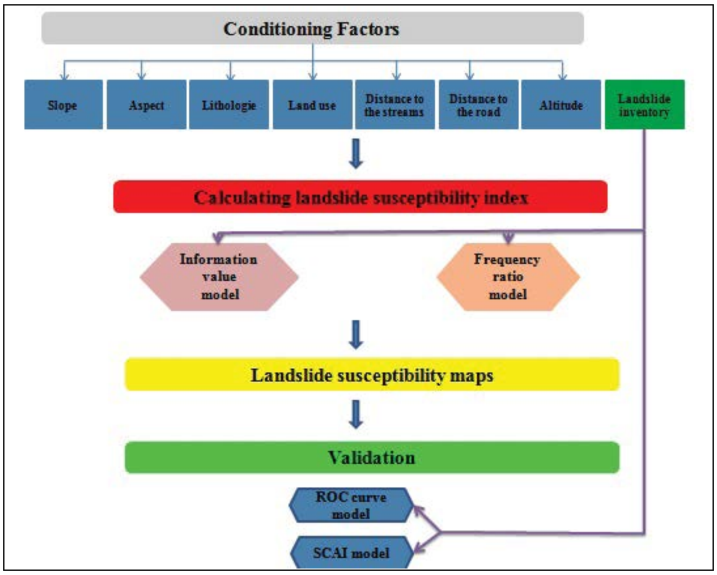

Figure 10- Methodology flowchart for the process work.

in a given class and the density of the same class. (Lee and Talib, 2005).LSI expressed using following Equation: (Equation 1)

$$LSI \quad Fr1 + Fr2 + Fr3 + ... + Frn \tag{1}$$

In the statistical analysis between landslide occurrence ratio and ratio of each class in conditioning factor, the average value of Fr is equal to 1. If the value is >1, indicate maximal correlation and a value lower than 1 present minimal correlation. Table 3 shows the results of this application.

As a result, for the slope degree, FR increased with increasing of the slope degree, the class (>50) has maximum value (3.995), while the class (0 – 10) has the minimum value (0.338). Aspect analyses show that the maximum FR value (3.454) is for Northwest, followed by West (2.573), North (2.025) and Flat (1.915), indicating the maximal probability of landslide occurrence. Frequency results of lithology parameter indicate that the gray marl, white marl-limestone, gypsum and dune marine with maximum FR value (10.397) are most prone to landslide. The FR values greater than 1 are distributed at the distance closer to the streams (0-100) and (100-200) indicating a high probability of landslide occurrence. For the proximity to the road give respectively, value 1.125, 1.507 and 1.710 for the distance (300 - 450), (450-600) and > 600. Correlation between land use and landslide indicate that the landslide commonly occurred in barren area (4.086) and maquis area (1.759). The combination between altitude and landslide inventory, showed that landslides mostly appeared from 0 to 100m.

Using equation 1, LSI values range from 1.15 to 27.13. Using reclassify function, the LSI map was reclassified into five classes: very low (39.07%), low (31.46%), moderate (19.80%), high (4.72%) and very high (4.93%) (Figure 11a-c).

5.2. Information Value Method

The statistical method used in this study is proposed by Yin and Yan, 1988 and modified by van Westen, 1993, is based on the comparison between the spatial distribution of phenomena and their various factors. First, the method is based on a statistical analysis using Equation (2)

$$W(i) = \frac{Npix(Si)/Npix(Ni)}{\sum Npix(si)/\sum Npix(Ni)} \tag{2}$$

W (i) is the weight of each class (for example the weight of class 10 ° of the slope), Npix (Si) is the number of slip pixels in classes i, Npix (Ni) is the number of pixels in class i. the dominator is the ratio between number of pixels all landslide and total pixels in the study area. In a second step, the probability of occurrence of landslides in each class is determined by Equation (3):

Table 3- Spatial relationship between each factor contributing to a landslide and the landslide using the FR and information value models.

Parametre	Classes	% of total area (a)	% of landslide area (b)	Frequency Ratio (b/a)	Information value (Wi)
Slope (°)	0-10	69.477	23.526	0.338	-1.102
	10-20	14.877	36.920	2.481	0.889
	20-30	09.710	23.138	2.382	0.848
	30-50	05.813	15.929	2.739	0.988
	>50	00.211	00.485	3.995	1.365
Aspect	Flat	00.042	0.0811	1.915	0.613
	North	11.744	23.792	2.025	0.669
	Northeast	14.347	10.149	0.705	-0.385
	East	15.546	02.908	0.187	-0.713
	Southwest	18.028	02.696	0.149	-1.937
	South	15.056	02.015	0.133	-2.047
	Southwest	08.081	05.734	0.709	-0.380
	West	07.409	19.066	2.573	0.908
	Northwest	09.712	33.554	3.454	1.202
Lithology	Class 1	55.022	03.612	0.065	-2.727
	Class 2	32.656	04.205	0.128	-2.053
	Class 3	03.462	00.075	0.021	-3.833
	Class 4	08.858	92.210	10.397	2.337
Distance to the stream	0-100	41.838	48.409	1.157	0.174
	100-200	22.937	26.137	1.139	0.159
	200-300	11.845	11.370	0.959	-0.012
	300-400	07.346	05.855	0.797	-0.198
	400-500	05.402	03.201	0.592	-0.494
	500-600	04.565	02.989	0.654	-0.394
	600-700	03.865	01.379	0.356	-2.414
	>700	02.198	00.656	0.298	-2.592
Land use	class1	10.469	07.164	0.684	-0.396
	class2	32.693	57.516	1.759	0.457
	class3	49.122	03.791	0.077	-1.119
	class4	07.714	31.527	4.086	1.390
Distance to the road	0-150	28.604	08.318	0.290	-1.251
	150-300	21.739	17.740	0.816	-0.219
	300-450	15.284	17.796	1.125	0.101
	450-600	10.137	15.283	1.507	0.394
	> 600	24.233	41.460	1.710	0.226
Altitude	0-100	28.062	66.072	2.354	0.843
	100-200	39.549	25.429	0.642	-0.454
	200-300	18.001	05.789	0.321	-1.147
	300-400	08.671	02.709	0.312	-1.176
	400-500	04.125	0000	000	000
	> 500	01.590	0000	000	000

$$Pr(i) = \ln \frac{Npix(Si)/Npix(Ni)}{\sum Npix(si)/\sum Npix(Ni)} \quad (3)$$

Finally, the landslides susceptibility index (LSI) of the terrain is determined by the sum of all factors (Equation 4) after the integration of the probability of occurrence of slips in each class.

$$LSI = \sum_{i=1}^{n} \ln \frac{Npix(Si)/Npix(Ni)}{\sum Npix(si)/\sum Npix(Ni)} \quad (4)$$

The combinations of the thematic maps with landslide inventory map in ArcGIS allow calculating the number of pixels of the landslide in each class. The information value method allowed us to calculate the weight of each class (Table 3). Positive and negative results of LSI mean that the highest values indicate a great possibility of sliding. The final calculated LSI values of the study area range from -11.98 to 7.53. The LSI map was classified into five classes using natural breaks (jenks) method (very low 19.12%, low 33.3%,

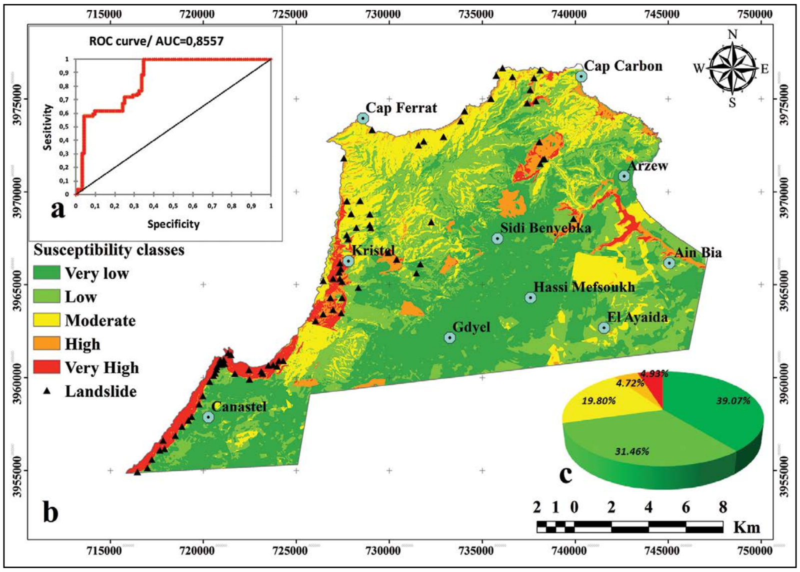

Figure 11- a) ROC curve of the LSM provide by frequency model, b) Landslide susceptibility map produced using frequency model, c) distribution pie-chart of the landslide susceptibility classes.

moderate 24.46%, high 18.34% and very high 4.75%) (Figure 12b, c).

5.3. Validation

For validation process, two statistical methods were used to evaluate the performance of the LSMs obtained. Both of ROC curve and SCAI methods are based on the combination of the landslide susceptibility and landslide inventory map. ROC curve have comparing 30% of landslides with the two LSMs. The AUC value was 85.57% for FR model (Figure 10a), and 89.03 for IV model (Figure 11a). Comparing the obtained results of Area under curve for the two models indicate that the use of the IV for landslide susceptibility zoning provide more accurate prediction in comparing the FR model .

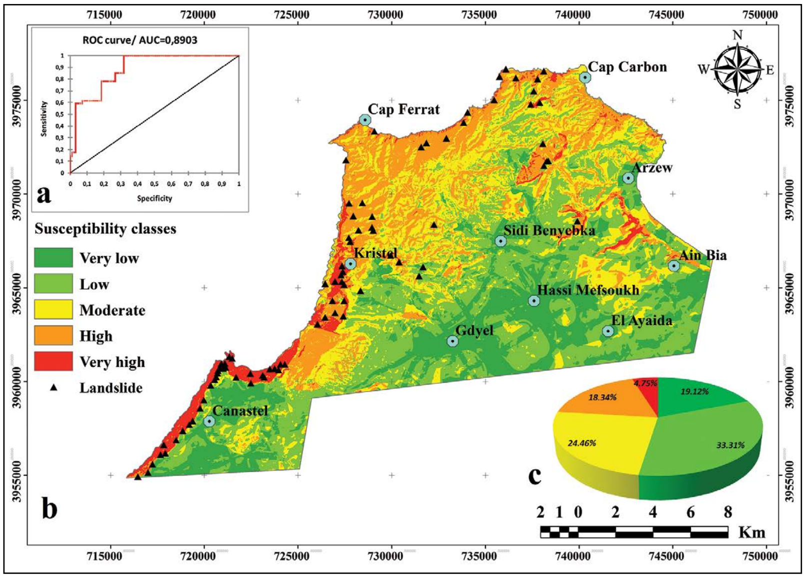

Figure 12- a) ROC curve of the LSM provide by bivariate statistical model, b) Landslide susceptibility map produced using information value model, c) Distribution pie-chart of the landslide susceptibility classes.

Oriented solution based about the SCAI method was proposed to compare the results of two methods according to the LSM. The SCAI method was cited by Süzen and Doyuran, 2004 as validation tool of landslide susceptibility map. In order to evaluate SCAI, we use the following Equation:

$$SCAI = \frac{SAP}{LP} \tag{5}$$

Were, SAP are the percentages of susceptibility area and LP is the percentage of landslide.

According to the table 4, very high and high classes have contained the minimum SCAI, for the low and very low classes contain maximal SCAI value. The obtained results of the SCAI method, confirmed that the IV method more performance than FR method .

Table 4- The densities of landslide occurrence among the landslide susceptibility classes for the two models.

Model	FR			IV		
Susceptibility classes	Area (%)	Seed (%)	SCAI	Area (%)	Seed (%)	SCAI
Very low	39,07	2,01	19,44	19.12	0.27	70.81
Low	31,46	2,5	12,58	33.31	2.08	16.01
Moderate	19,8	3,33	5,95	24.46	4.80	5.09
High	4,72	5,7	0,83	18.34	10.68	1.71
Very high	4,93	86,44	0,06	4.75	82.15	0.05

6. Conclusion

Geological risk, related to landslide presented a strong danger for the socio-economic of regions located in North part of Algeria; however, the investigations about the landslide problem in Algeria which have already been published are rare and scattered. In recent literature a few attempt at landslide were applied in the North eastern of Algeria. The present study confirmed that the North western of Algeria was also suffered from slope movement problem. The selected region was lacked a precondition studies, maps and documents to define landslide prone area and mitigate landslide consequences.

In this article, two landslide susceptibility maps of the Arzew sector North western of Algeria were established. The FR and VI methods were used to define relationship between landslides spatial distribution and the predisposing factors.

The AUC results using ROC curve indicate that the use of information value model (89.03%) for established LSM provide more accurate prediction in comparing with frequency ratio (85.57%).

In other hand, the results of Seed Cell Area Index (SCAI) model, also confirmed that the landslide susceptibility map elaborate by the information value method is more accurate than the other model used in this work.

Mapping field susceptible of the landslides for the Arzew area can be evaluated by the use of other models and it can be developed by the combination of many others data.

The proposed models experimented can be considered as a powerful tool for decision makers to the revision of the PDAU (master plan of planning and development), furthermore, this document may serve local communities and planners in choosing suitable locations for future projects and take preventive measures about landslide prone area (high and very high landslide susceptibility classes).

Acknowledgements

This research was supported by University Oran 2 Mohamed Benahmed, Algeria. The authors are grateful to the Organizing Committee of ISEMG 2018 and to Professor M. Gürhan Yalçın, Professor Hamidi Mansour and Professor Hassani Moulay Idris for their valuable comments and suggestions. The authors would to like to thanks the anonymous reviewers for their constructive comments of this work.

References

Achour, Y., Boumezbeur, A., Hadji, R., Chouabbi, A., Cavaleiro, V., Bendaoud, E. A. 2017. Landslide susceptibility mapping using analytic hierarchy process and information value methods along a highway road section in Constantine, Algeria. Arabian Journal of Geosciences 10:194.

Aghdam, I., N., Varzandeh, M.H.M., Pradhan, B. 2016. Landslide susceptibility mapping using an ensemble statistical index (Wi) and adaptive neuro-fuzzy inference system (ANFIS) model at Alborz Mountains (Iran). Environmental Earth Sciences 75:553.

Akgün, A., Dağ, S., Bulut, F. 2008. Landslide susceptibility mapping for a landslide-prone area (Findikli, NE of Turkey) by likelihood-frequency ratio and weighted linear combination models. Environmental Geology 54:1127-1143.

Bai, S., Lü, G., Wang, J., Zhou, P., Ding, L. 2011 GIS-based rare events logistic regression for landslide-susceptibility mapping of Lianyungang, China. Environmental Earth Sciences 62:139-149.

Ballabio, C., Sterlacchini, S. 2012. Support vector machines for landslide susceptibility mapping: the Staffora River Basin case study, Italy. Mathematical geosciences 44:47-70

Benabdellah, M. 2010. Mis en évidence des phénomènes contrôlant le littoral oranais (de la Calère a la pointe de Canastel) : étape fondamentale pour une cartographie des risques géologiques. Mémoire de magister, Université d'Oran, 258p.

Benaissa, A., Cordary, D., Gioraud, A. 1989. Les mouvements de terrain dans la zone urbaine de Constantine (Algérie). Bulletin of the International Association of Engineering Geology-Bulletin de l'Association Internationale de Géologie de l'Ingénieur 40:85-90

Beneder. 2011. Carte d'occupation du sol wilaya d'Oran notice explicative. Bureau national d'études pour le développement rural, Rapport inédite, 13p.

Bourenane, H., Bouhadad, Y., Guettouche, MS., Braham, M. 2015. GIS-based landslide susceptibility zonation using bivariate statistical and expert approaches in the city of Constantine (Northeast Algeria). Bulletin of Engineering Geology and the Environment 74:337-355.

Bui, D.T., Lofman, O., Revhaug, I., Dick, O. 2011. Landslide susceptibility analysis in the Hoa Binh province of Vietnam using statistical index and logistic regression. Natural Hazards 59:1413.

Chen, W., Li, W., Chai, H., Hou, E., Li, X., Ding, X. 2016. GIS-based landslide susceptibility mapping using analytical hierarchy process (AHP) and certainty factor (CF) models for the Baozhong region of Baoji City, China. Environmental Earth Sciences 75:63.

Chen, W., Pourghasemi, H. R., Zhao, Z. 2017. A GIS-based comparative study of Dempster-Shafer, logistic regression and artificial neural network models for landslide susceptibility mapping. Geocarto International 32:367-385.

Ciszak, R. 1993. Evolution géodynamique de la chaîne tellienne en Oranie (Algérie occidentale) pendant le Paléozoïque et le Mésozoïque vol 20. Laboratoire de géologie sédimentaire et paléontologie, Thèse de doctorat, Université Paul Sabatier, 513p.

Conforti, M., Pascale, S., Robustelli, G., Sdao, F. 2014. Evaluation of prediction capability of the artificial neural networks for mapping landslide susceptibility in the Turbolo River catchment (northern Calabria, Italy). Catena 113:236-250.

Corominas, J., Van Westen, C., Frattini, P., Cascini, L., Malet, J. P., Fotopoulou, S., Catani, F., Van DenEeckhaut, M., Mavrouli, O., Agliardi, F., Pitilakis, K., Winter, M.G., Pastor, M., Ferlisi, S., Tofani, V., Herva´s, J., Smith, J.T., 2014. Recommendations for the quantitative analysis of landslide risk. Bulletin of Engineering Geology and the Environment 73, 209–263.

Cruden, D.M, Varnes, D.J. 1996. Landslide Types and Processes, Special Report, Transportation Research Board, National Academy of Sciences, 247: 36-75.

Cui, K., Lu, D., Li, W. 2016. Comparison of landslide susceptibility mapping based on statistical index, certainty factors, weights of evidence and evidential belief function models. Geocarto International:1-21.

Dahoua, L., Yakovitch, S., Hadji, R. 2017.GIS-based technic for roadside-slope stability assessment: an bivariate approach for A1 East-West highway, North Algeria. Mining Science 24.

Djerbal, L., Khoudi, I., Alimrina, N., Melbouci, B., Bahar, R. 2017 Assessment and mapping of earthquake-induced landslides in Tigzirt City, Algeria. Natural Hazards:1-21.

Djerbal, L., Melbouci, B. 2013. Contribution to the mapping of the landslide of Aïn El Hammam (Algeria). In: Advanced Materials Research,. Trans Tech Publ, pp 332-336.

Ercanoğlu, M., Kasmer, O., Temiz, N. 2008. Adaptation and comparison of expert opinion to analytical hierarchy process for landslide susceptibility mapping. Bulletin of Engineering Geology and the Environment 67:565-578.

Fell, R., Corominas, J., Bonnard, C., Cascini, L., Leroi, E., Savage, WZ. 2008 .Guidelines for landslide susceptibility, hazard and risk zoning for land use planning. Engineering Geology 102:85-98.

Fenet, B. 1975. Recherches sur l'alpinisation de la bordure septentrionale du Bouclier africain à partir de l'étude d'un élément de l'orogène nord-maghrébin : les monts du Djebel Tessala et les massifs du littoral oranais, Thèse de doctorat, Université de Nice, 310p.

Ghosh, K., Bandyopadhyay, S., De, S.K. 2017. A Comparative Evaluation of Weight-Rating and Analytical Hierarchical (AHP) for Landslide Susceptibility Mapping in Dhalai District, Tripura. In: Environment and Earth Observation. Springer, pp 175-193.

Gomes, A., Gaspar, J., Goulart, C., Queiroz, G. 2005. Evaluation of landslide susceptibility of Sete Cidades Volcano (S. Miguel Island, Azores). Natural Hazards and Earth System Science 5:251-257.

Gorsevski, P.V., Gessler, P.E., Boll, J., Elliot, W.J., Foltz, R.B. 2006*a*. Spatially and temporally distributed modeling of landslide susceptibility. Geomorphology 80:178-198.

Gorsevski, P.V., Gessler, P.E., Foltz, R.B., Elliot, W.J. 2006*b*. Spatial prediction of landslide hazard using logistic regression and ROC analysis. Transactions in GIS 10:395-415.

Gorsevski, P.V., Jankowski, P., Gessler, P.E. 2006*c*. An heuristic approach for mapping landslide hazard by integrating fuzzy logic with analytic hierarchy process. Control and Cybernetics 35:121-146.

Gourinard, Y. 1952*a*. Carte géologique détaillée de l'Algérie. Feuille Arzew (127) 2ème idition, Serv. Carte Géol. Alger, Algérie.

Gourinard, Y. 1952*b*. Carte géologique détaillée de l'Algérie. Feuille Oran (159) 2ème idition, Serv. Carte Géol, Alger, Algérie.

Guemache, M.A., Chatelain, J.L., Machane, D., Benahmed, S., Djadia, L. 2011. Failure of landslide stabilization measures: the Sidi Rached viaduct case (Constantine, Algeria). Journal of African Earth Sciences 59:349-358.

Guzzetti, F., Reichenbach, P., Cardinali, M., Galli, M., Ardizzone, F. 2005. Landslide hazard assessment in the Staffora basin, northern Italian Apennines. Geomorphology 72:272-299.

Hadji, R., Boumazbeur, A., Limani, Y., Baghem, M., el Madjid Chouabi, A., Demdoum, A. 2013. Geologic, topographic and climatic controls in landslide hazard assessment using GIS modeling: a case study of Souk Ahras region, NE Algeria. Quaternary International 302:224-237.

Hadji, R., Limani, Y., Demdoum, A. 2014. Using multivariate approach and GIS applications to predict slope instability hazard case study of Machrouha municipality, NE Algeria. In: Information and Communication Technologies for Disaster Management (ICT-DM), 1st International Conference on, 2014. IEEE, pp 1-10.

Hadji, R., Rais, K., Gadri, L., Chouabi, A., Hamed, Y. 2017. Slope failure characteristics and slope movement susceptibility assessment using GIS in a medium scale: a case study from Ouled Driss and Machroha municipalities, Northeast Algeria. Arabian Journal for Science and Engineering 42:281-300.

Intarawichian, N., Dasananda, S. 2010. Analytical Hierarchy Process For Landslide Susceptibility Mapping In Lower Mae Chaem Watershed, Northern Thailand. Suranaree Journal of Science & Technology 17.

Lee, S., Talib, J.A. 2005. Probabilistic landslide susceptibility and factor effect analysis Environmental geology 47:982-990

Mahdadi, F., Boumezbeur, A., Hadji, R., Kanungo, D.P., Zahri, F. 2018. GIS-based landslide susceptibility assessment using statistical models: a case study from Souk Ahras province, NE Algeria. Arabian Journal of Geosciences 11:476

Özdemir, A., Altural, T. 2013. A comparative study of frequency ratio, weights of evidence and logistic regression methods for landslide susceptibility mapping: Sultan Mountains, SW Turkey. Journal of Asian Earth Sciences 64:180-197.

Peng, L., Niu, R., Huang, B., Wu, X., Zhao, Y., Ye, R. 2014. Landslide susceptibility mapping based on rough set theory and support vector machines: A case of the Three Gorges area, China. Geomorphology 204:287-301.

Perrodon, A. 1957. Etude géologique des bassins néogènes sublittoraux de l'Algérie occidentale. Thèse de doctorat, Université d' Oran, 301p.

Pourghasemi, H., Moradi, H., Aghda, S.F. 2013. Landslide susceptibility mapping by binary logistic regression, analytical hierarchy process, and statistical index models and assessment of their performances. Natural Hazards 69:749-779.

Pradhan, B. 2011. Manifestation of an advanced fuzzy logic model coupled with Geo-information techniques to landslide susceptibility mapping and their comparison with logistic regression modeling. Environmental and Ecological Statistics 18:471-493.

Pradhan, B., Jebur, M.N., Abdullahi, S. 2017. Spatial Prediction of Landslides Along Jalan Kota in Bandar Seri Begawan (Brunei) Using Airborne LiDAR Data and Support Vector Machine. Laser Scanning Applications in Landslide Assessment. Springer, pp 167-178.

Raja, NB., Çiçek, I., Türkoğlu, N., Aydın, O., Kawasaki, A. 2017. Landslide susceptibility mapping of the Sera River Basin using logistic regression model. Natural Hazards 85:1323-1346.

Regmi, N.R., Giardino, J.R., Vitek, J.D. 2010. Modeling susceptibility to landslides using the weight of evidence approach: Western Colorado, USA. Geomorphology 115:172-187.

Sezer, E.A., Pradhan, B., Gökçeoğlu, C. 2011. Manifestation of an adaptive neuro-fuzzy model on landslide susceptibility mapping: Klang valley. Malaysia Expert Systems with Applications 38:8208-8219.

Süzen, M., Doyuran, V. 2004. A comparison of the GIS based landslide susceptibility assessment methods: multivariate versus bivariate. Environmental geology 45:665-679.

Thiery, Y. 2007. Susceptibilité du Bassin de Barcelonnette (Alpes du Sud, France) aux'mouvements de versant': cartographie morphodynamique, analyse spatiale et modélisation probabiliste. Thèse de doctorat, Université de Caen, 445p.

Thomas, G. 1985. Géodynamique d'un bassin intramontagneux Le bassin du Bas Chélif occidental (Algérie) durant le Mio-Plio-Quaternaire. Thèse de doctorat, Université de Pau, 594p.

Van Westen, C. J. 1993. Application of geographic information systems to landslide hazard zonation. ITC Publication, Vol.15. International Institute for Aerospace Survey and Earth Sciences, Enschede 245pp.

Yalçın, A., Reis, S., Aydınoğlu, A., Yomralıoğlu, T. 2011. A GIS-based comparative study of frequency ratio, analytical hierarchy process, bivariate statistics and logistics regression methods for landslide susceptibility mapping in Trabzon, NE Turkey. Catena 85:274-287.

Yeşilnacar, E., Topal, T. 2005. Landslide susceptibility mapping: a comparison of logistic regression and neural networks methods in a medium scale study, Hendek region (Turkey). Engineering Geology 79:251-266.

Yılmaz, I. 2009. A case study from Koyulhisar (Sivas-Turkey) for landslide susceptibility mapping by artificial neural networks Bulletin of Engineering Geology and the Environment 68:297-306.

Yılmaz, I. 2010. Comparison of landslide susceptibility mapping methodologies for Koyulhisar, Turkey: conditional probability, logistic regression, artificial neural networks, and support vector machine. Environmental Earth Sciences 61:821-836.

Yin, K., Yan, T. 1988. Statistical prediction model for slope instability of metamorphosed rocks. In: Proceedings of the 5th International Symposium on Landslides. sl]:[sn], pp 1269-1272.

Youssef, A.M., Al-Kathery, M., Pradhan, B. 2015. Landslide susceptibility mapping at Al-Hasher area, Jizan (Saudi Arabia) using GIS-based frequency ratio and index of entropy models. Geosciences Journal 19:113-134.